Resource-Efficient Technologies 3 (2017) 506–515

Contents lists available at ScienceDirect

Resource-Efficient Technologies

journal homepage: www.elsevier.com/locate/reffit

Research paper

Green synthesis of silver nanoparticles using *Lippia nodiflora* aerial extract and evaluation of their antioxidant, antibacterial and cytotoxic effects

Arumugam Sudha[a], Jeyaraman Jeyakanthan[a], Pappu Srinivasan[b,*]

[a] Department of Bioinformatics, Alagappa University, Karaikudi 630003, Tamil Nadu, India
[b] Department of Animal Health and Management, Alagappa University, Karaikudi 630003, Tamil Nadu, India

ARTICLE INFO

Article history:
Received 23 January 2017
Revised 9 July 2017
Accepted 31 July 2017
Available online 14 August 2017

Keywords:
Lippia nodiflora
Silver nanoparticles
SEM
Antioxidant
Antibacterial
Cytotoxicity

ABSTRACT

Silver nanoparticles biosynthesis has received increasing attention in the field of nanotechnology due to their antimicrobial and biomedical applications. Green synthesis of metal nanoparticles is anticipated as a cost effective and eco-friendly alternative in the current research scenario. With this aim, the aqueous extracts made from the aerial parts of *Lippia nodiflora* were used as the reducing agents to synthesize silver nanoparticles (AgNPs) and their antioxidant, antibacterial and cytotoxic properties have also been evaluated. The biosynthesized AgNPs were characterized by UV–Visible Spectroscopy, Fourier-Transform Infrared Spectroscopy (FTIR) and X-Ray Diffraction (XRD) analysis. The AgNPs were found to be stable at −25.2 mV through zeta potential study. The morphology and size of synthesized silver nanoparticles were confirmed by Scanning Electron Microscope with energy dispersive spectra (SEM-EDX) and Transmission Electron Microscopy (TEM) analysis with size range from 30 to 60 nm. Biosynthesized AgNPs exhibited strong antioxidant activity as well as showed potent antibacterial activity against human pathogenic bacteria. The cytotoxicity study of AgNPs was also revealed against MCF-7 breast cancer cell lines in a dose-dependent manner. The recognized bioactivity confirmed by the synthesized AgNPs directs towards the clinical use as an antioxidant, antibacterial and cytotoxic agent.

1. Introduction

Nanotechnology is one of the most interesting areas of research in this era, which is budding day by day, with an impact in diverse aspects of human life [1]. For the past few years, nanometallic particles are gaining much attention owing to their applicability in the field of medicines, biology, material sciences and electronics at the nanoscale level [2]. Even though several routes are accessible, the synthesis of nanoparticles with a biological approach turns out to be crucial [3]. In the present scenario, the biosynthesis of nanoparticles using plant extracts are much simpler than the chemical synthesis method and may be employed for several therapeutic applications [4,5]. Moreover, the synthesis of nanoparticles using the plant extract as a reducing and capping agent was more beneficial than microbial synthesis. The effects of diverse plants like *Ficus carica* [6], *Piper longum* [7], *Rosmarinus officinalis* [8], *Lantana camara* [9], *Prunus yedoensis* [10], *Zingiber officinale* [11] *Azadirachta indica* [12], *Erythrina indica* [13], beet root [14], etc., were also reported for the synthesis of various metal nanoparticles.

Antioxidants are very essential to protect cells and biological macromolecules from degenerative reactions produced by free radicals and reactive oxygen species [15]. The antioxidant property of various plant products, such as polyphenolic substances (*e.g.*, flavonoids and tannins) derived from various plants and herbal extracts have been reported [16–18]. In recent studies, the oxygen-based free radicals have been proved to be scavenged effectively by inorganic nanoparticles [19,20]. Moreover, silver has long been documented as a valuable antimicrobial agent that reveals low toxicity in humans and comprises various *in vitro* and *in vivo* applications among the other metals [21]. The highly reactive metal oxide nanoparticles are well known to demonstrate tremendous bactericidal activity against Gram-positive and Gram-negative bacteria [22]. Recently, AgNPs exhibit lot of scope in the field of high sensitivity biomolecular detection, catalysis, biosensors and medicine along with the anti-fungal, anti-inflammatory and anti-angiogenesis activities [23,24]. In addition to antioxidant and antimicrobial activity, the cytotoxicity studies also comprise promi-

* Corresponding author.
E-mail address: sri.bioinformatics@gmail.com (P. Srinivasan).

http://dx.doi.org/10.1016/j.reffit.2017.07.002

nent significance and numerous studies are underway to elucidate these aspects.

In Indian traditional medicine, herbal extracts have long been used for treating varied pathological processes including respiratory, neurodegenerative and cardiovascular ailments [25,26]. Thus, nanoparticles synthesized by using such herbal extract may perhaps serve together as bactericidal and antioxidants. In the present study, we have explored the biosynthesis of AgNPs using the aqueous extract of aerial parts of *Lippia nodiflora. L. nodiflora* (Verbenaceae), a crawling recurrent herb, grow up in maritime areas near rivers and found throughout India. The plant exhibits anodyne, cardiotonic, antibacterial, diuretic, parasiticide and refrigerant properties [27]. Several studies regarding pharmacological properties of aerial parts of *L. nodiflora* were reported. However, till date, there is no report that portrays its prospective in nanobiotechnology to synthesize nanoparticles and thereby assessing its biomedical efficacy. Hence the present study was carried out to synthesize and characterize silver nanoparticles and to examine their antioxidant and antibacterial activities. In addition, the cytotoxic effect of green synthesized AgNPs against MCF-7 breast cancer cell line was also determined.

2. Materials and methods

2.1. Reagents

The reagents such as silver nitrate ($AgNO_3$), 2-Deoxy-D-ribose, butylated hydroxyl toluene (BHT), 2, 2-diphenyl-1-picrylhydrazyl (DPPH), phenazine methosulphate (PMS), nitroblue tetrazolium (NBT), MTT [3-(4, 5-dimethylthiazol- 2-yl)-2, 5-diphenyltetrazolium bromide] were obtained from (Sigma Chemicals St. Louis, MO, USA). 2, 4,6- tripyridyl- S- triazine (TPTZ), thiobarbituric acid (TBA), trichloroacetic acid (TCA) ethylene diaminetetraacetic acid (EDTA), ferric chloride ($FeCl_3$), hydrogen peroxide (H_2O_2), and nicotinamide adenine dinucleotide-reduced (NADH), were obtained from M s^{-1} (Sisco Research laboratories, Mumbai, India). Nutrient agar and broth for antimicrobial activity were purchased from Hi-Media, Mumbai, India. All other chemicals and reagents used in this study were of analytical grade.

2.2. Preparation of L. nodiflora aerial extract

The fresh aerial parts of *L. nodiflora* were collected from Karaikudi, Sivagangai District, Tamilnadu and its identification was confirmed by a taxonomist, as reported earlier [28]. The freshly collected plant material was washed thoroughly with tap water, shade dried for 2 weeks at room temperature and then powdered with kitchen blender. The aerial parts of *L. nodiflora* exhibit highest polyphenolic content (98.31 ± 0.004 mg GAE/g), determined using the standard curve of gallic acid. In the present study, 10 g of powder was taken and mixed with 100 ml of sterilized double distilled water and boiled in a water bath at 60 °C for 10 min. After cooling, the mixture was filtered with Whatman No.1 filter paper and the aqueous filtrate was used for further study.

2.3. Biosynthesis of AgNPs

For the biosynthesis of AgNPs, 10 ml of aqueous extract was added to 190 ml of 1 mM aqueous silver nitrate solution and the synthesis was carried out using the conical flask. The mixture was gradually boiled in a water bath at varying temperatures ranging from 30 to 95 °C for 10 min, in order to study the temperature effects on the synthesis rate of AgNPs. Reduction of silver nanoparticles was observed by change in their color of the reaction mixture during temperature treatment. A control setup was also maintained without *L. nodiflora* extract. The AgNPs solution were subsequently purified by repeated centrifugation at 10,000 rpm for 20 min at 4 °C and the pellet obtained was suspended in sterilized double distilled water and freeze dried using lyophilizer.

2.4. Characterization of AgNPs

An aliquot of synthesized nanoparticles was initially characterized by UV–visible spectrophotometer in the wavelength range of 300–700 nm with Shimadzu spectrophotometer (Model UV-1800, Shimadzu, Kyoto, Japan) operating at 1 nm resolution. Fourier transform infrared spectroscopy (FTIR) analysis was carried out on Bruker Tensor 27 instrument (Germany) and the spectra were recorded in the range of wavelength between 4000 cm^{-1} and 400 cm^{-1}. For comparison, UV–visible and FTIR spectral analysis was also performed to the extract before addition of the silver nitrate solution. For XRD studies, dried nanoparticles were coated on XRD grid and the spectra was recorded using Cu Kα radiation ($\lambda = 1.54060$ Å) with nickel monochromator in the range of 2θ from 10° to 80°. The average crystalline size of the synthesized AgNPs was calculated using Scherrer's formula ($D = 0.9\lambda/\beta\cos\theta$). A small portion of AgNPs suspension was placed on glass slide to make thin film, dried over hot air oven and then the thin film was used for the SEM analysis equipped with EDX (SEM FEI QUANTA 250). The particle size distribution of AgNPs was evaluated using dynamic light scattering (DLS) measurements and zeta potential analysis was conducted with a Malvern Zetasizer Nanoseries compact scattering spectrometer (Malvern Instruments Ltd., Malvern, UK). The AgNPs were dissolved in physiological saline (0.9% w/v of NaCl) for zeta potential analysis. Data obtained were analyzed using Zetasizer software. The shape and size of the particles were measured with transmission electron microscopy (TEM) using Tecnai 10 instrument at 120 kV.

2.5. Determination of antioxidant activities

2.5.1. DPPH radical scavenging assay

The DPPH radical scavenging activity of silver nanoparticles was determined, as previously described [29]. Different concentrations (25–500 µg/ml) of AgNPs were prepared in de-ionized water and 0.1 ml of AgNPs solution was added to 1 ml of 0.1 mM of freshly prepared DPPH solution in ethanol. The reaction mixtures were shaken vigorously and absorbance at 517 nm was determined after 20 min at room temperature. Control sample was prepared without silver nanoparticles. BHT was used as positive control in all the assays. The radical scavenging activity was measured as a decrease in the absorbance of $DPPH^{\bullet}$ and calculated as follows:

$$\text{Scavenging effect}\ (\%) = [(A_c - A_s)/A_c] \times 100$$

where, A_c is the absorbance of the control, and A_s is the absorbance of the sample or standard.

2.5.2. Superoxide anion radical-scavenging assay

The superoxide anion radical-scavenging effect was determined by the method of Nishikimi et al. [30]. The purple formazan formed by nitroblue tetrazolium (NBT) by reacting with the superoxide radicals produced from phenazine methosulfate–nicotinamide adenine dinucleotide (PMS/NADH) non-enzymatic system was measured spectrophotometrically. In this assay, the reaction mixture consists of NBT (1 mM) in phosphate buffer (0.1 M, pH 7.4), NADH (1 mM), PMS (0.1 mM) and different concentrations (25–500 µg/ml) of AgNPs was incubated at room temperature for 5 min and the absorbance was recorded at 560 nm. The inhibition percentage was calculated against a control without the sample. The scavenging ability was calculated using the equation as described for DPPH assay.

2.5.3. Measurement of reducing power

The reducing power was determined by the method of Yen and Chen, [31]. In brief, various concentrations of AgNPs solution (25–500 µg/ml) were prepared and 0.1 ml of the sample solutions was mixed with sodium phosphate buffer (0.2 M, pH 6.6) and 1% potassium ferricyanide (1 g/100 ml water). The reaction mixture was incubated at 50 °C for 20 min and then cooled rapidly. After incubation, 10% trichloroacetic acid (w/v) was added to terminate the reaction followed by centrifugation at 3000 rpm for 10 min. The supernatant was mixed with 0.1% ferric chloride, and the absorbance was measured spectrophotometrically at 700 nm. The obtained results were compared with BHT which was used as a positive control. Higher absorbances of the resultant solution designate a higher reducing activity.

2.5.4. Measurement of hydrogen peroxide scavenging activity

The ability of AgNPs to scavenge hydrogen peroxide (H_2O_2) was determined according to the method of Ruch et al. [32] with slight modifications. Briefly, different concentrations of AgNPs (25–500 µg/ml) and BHT was mixed with 2.4 ml of phosphate buffer (0.1 M, pH 7.4) and 0.6 ml of H_2O_2 solution (40 mM), vortexed and incubated at room temperature for 10 min. At the end of incubation, the concentration of hydrogen peroxide was determined by absorption at 230 nm against a blank solution containing phosphate buffer without hydrogen peroxide. The H_2O_2 scavenging ability was calculated using the formula as described for DPPH assay.

2.5.5. Hydroxyl radical scavenging assay

The capacity of AgNPs to reduce hydroxyl radical-mediated peroxidation was carried out by the method of Hinneburg et al. [33]. Briefly, 0.5 ml of 5.6 mM 2-deoxy-D-ribose in KH_2PO_4–NaOH buffer (50 mM, pH 7.4), 0.2 ml of 100 µM $FeCl_3$ and 104 mM EDTA (1:1 v/v) solution were added to 0.1 ml of different concentrations of AgNPs solution (25–500 µg/ml), followed by addition of 100 µl of 1.0 mM H_2O_2 and 0.1 ml of 1.0 mM aqueous BHT. The reaction mixtures were shaken vigorously and incubated at 50 °C for 30 min. Subsequently, 1 ml of 2.8% TCA and 1 ml of 1% TBA were added to each tube containing reaction mixture and samples were mixed well again and boiled in a water bath at 50 °C for 30 min. The reaction mixture without sample was used as the control. The absorbance of solution was read at 532 nm. The hydroxyl radical scavenging ability was calculated using the formula as described for DPPH assay.

2.6. Antibacterial activity of biosynthesized nanoparticles

The antibacterial activity of synthesized AgNPs and *L. nodiflora* aqueous extract were determined by disc diffusion method against human pathogens such as *Staphylococcus aureus* (MTCC96), *Streptococcus mutans* (MTCC896), *Streptococcus pneumonia* (MTCC1936), *Escherichia coli* (MTCC40) and *Klebsiella pneumonia* (MTCC7407). These strains were obtained from Dr. N. M. Prabhu, Department of Animal Health and Management, Alagappa University, Karaikudi, Tamilnadu. The bacterial cultures were maintained at −80 °C in glycerol stock and were sub-cultured in nutrient broth for 24 h at 30 °C. Then each strain was spread uniformly into the individual nutrient agar plates. Sterile Whatman filter paper discs of 5 mm diameter were impregnated with AgNPs/plant extract (50 µg/ml) using sterile micropipette, and it was allowed to dry. The nanoparticles loaded discs along with control disc (without nanoparticles) were placed on the nutrient agar plates. After 24 h incubation at 37 °C, the zone of inhibition was measured and the assays were performed in triplicate.

2.7. Cell culture

MCF-7 cell line was purchased from National Center for Cell Sciences (NCCS), Pune, India. The cell line was cultured in the Dulbecco's Modified Eagles medium (DMEM) supplemented with 10% fetal bovine serum (FBS), 200 mM L-gulutamine, 100 U/ml penicillin, and 10 mg/ml streptomycin in a humidified atmosphere consisting of 5% CO_2 at 37 °C.

2.7.1. Evaluation of cytotoxicity

The cytotoxic effect of biosynthesized AgNPs against MCF-7 cells was evaluated by MTT [3-(4, 5- dimethylthiazol-2-yl)-2, 5-diphenyl tetrazolium bromide] assay. Briefly, MCF-7 cells were seeded (5×10^4 cells/well) in a 96-well plate and kept in CO_2 incubator for 24 h for attachment and growth. Then, the cells were treated with different concentration of biosynthesized AgNPs (5–100 μg/ml) and incubated for 24 h After incubation, the culture medium was removed and 15 μl of the MTT solution (5 mg/ml in PBS) was added to each well. Following 4 h incubation in dark, MTT was discarded and the resulting formazan crystals were solubilized in DMSO (100 μl/well). The absorbance was measured colorimetrically at 570 nm with an ELISA microplate reader. The percentage of cell viability was calculated using the following formula and expressed as IC_{50}.

$$= \frac{\text{OD value of treated cells}}{\text{OD value of untreated cells (control)}} \times 100$$

2.8. Statistical analysis

All statistical analyses were performed using GraphPad Prism 5.0 software (GraphPad Software, San Diego, CA, USA). Data signify the means plus or minus the standard deviation (mean ± SD) and are representative of three independent experiments.

3. Results and discussion

3.1. Characterization of AgNPs

The aerial parts of *L. nodiflora* were materialized to be a potential source of phytoconstituents to treat various diseases. It has been reported that the aerial parts contains various organic compounds such as alkaloids, flavonoids, steroids, phenols, glycosides and terpenoids [34,35]. The soluble components present in aqueous extract of *L. nodiflora* might found to be accountable for reduction of metal ions and stabilization of nanoparticles. The synthesis of AgNPs at varying temperatures denotes the color of the extract changes gradually from yellow to reddish-brown (inset), but the intensity of reddish-brown color developed was elevated at 95 °C, compared to other temperatures such as 30 °C, 60 °C and 90 °C (Fig. 1). From the obtained results, it was determined that AgNPs prepared were not aggregate, and were stable for one week at room temperature. Some research findings showed longer stability than one week for syntheses of AgNPs, which supported our research [36,37]. In the current study, the spectral peak of corresponding temperatures confirmed the maximum synthesis of AgNPs at 95 °C, by supporting a prominent color change. A fairy sharp and proportioned surface plasmon resonance (SPR) band width was observed at 442 nm for AgNPs prepared at 95 °C. Moreover, the comparison of UV-visible spectra shows that, the SPR band shifts from ≈475 nm at 30 °C to lower wavelengths (442 nm) at 95 °C, as the temperature increases. The obtained result may be ascribed to the size of particles range of 2 nm to 100 nm with spherical shape [38–40]. But, the UV-visible spectrum indicated no absorption in the range of 260–800 nm, before thermal reduction. The precise SPR arrangement of nanoparticle and absorbance depends on a

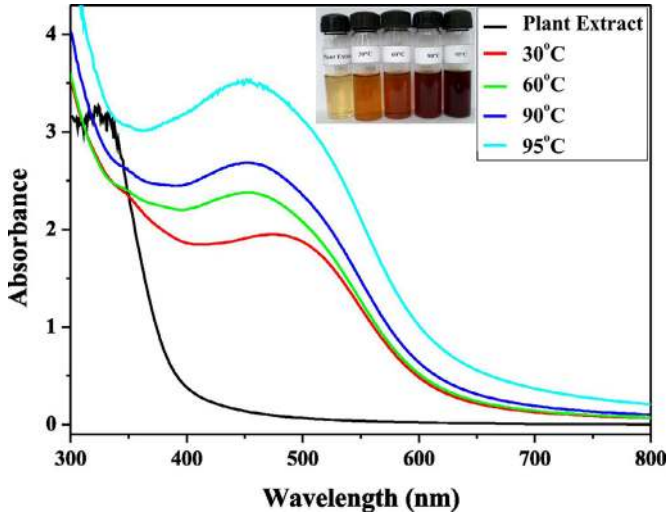

Fig. 1. UV–visible spectra of AgNPs synthesized using *L. nodiflora* extract at different temperatures.

number of sources such as the dielectric constant, pH, and temperature of the medium and particle size [41]. Therefore, the single SPR band as visualized by UV-visible analysis corresponds to the absorption spectra of spherical nanoparticles.

FTIR measurements were carried out to identify the promising biomolecules in the *L. nodiflora* aqueous extract accountable for the reduction of the silver ions and also the capping agent liable for the stability of the bioreduced AgNPs. The representative FTIR spectra of aqueous extract of *L. nodiflora* and obtained AgNPs of various temperatures were recorded and the major peaks are manifested in Fig. 2. The FTIR spectrum of the aerial extract showed sharp peaks at 3449, 1637, 1389, 1122, and 614 cm^{-1} (Fig. 2a) and also showed minor peaks at 2086, 1195, 1047 and 528 cm^{-1}. Whereas the biosynthesized AgNPs at different temperatures showed peaks in the 3400–3500, 2000–2100, 1600–1700, 1100–1200, and 600–700 cm^{-1} regions (Fig. 2b-e). There is no significant variation was observed among the spectral positions of peaks of biosynthesized AgNPs at different temperatures. The prominent band attributed at 3437–3452 cm^{-1} corresponds with the OH stretching of phenolic groups [42], the narrow band at 1636–1637 cm^{-1} can be attributed to C=O stretching probably due to the presence of amide group, which is accountable for the reduction of Ag^+ ions to AgNPs. The band at 2071–2086 cm^{-1} corresponds with the C–N stretching of any R–N=C=S and the band at 1086–1122 cm^{-1} were assigned to strong C–N stretching vibrations of aliphatic amines. The spectra illustrate the disappearance of bands at 1047, 1195, 1389 cm^{-1} and appearance of band at 636–688 cm^{-1} in the presence of AgNPs. The disappearance of band can be predictable to the vibrational stretching modes C–O–C of phenolic compounds at 1047 cm^{-1} [43] and C–O stretching (alcohols) at 1389 cm^{-1}. The appearance of peak may perhaps be due to the O–H bends correlated to phenolic elements of the plant [38]. The FT-IR analysis suggested that the reasonable mechanism of AgNPs formation may be due to the reduction of Ag^+ ions that takes place together with oxidation of phenolic components of polyols [44]. The nanoparticles prepared at 95 °C were used for further analysis based on intensity of color change and UV-vis predictions.

Fig. 3 shows the typical XRD pattern of biosynthesized AgNPs. The presence of characteristic of four diffraction peaks were observed at 38.04° (111), 44.23° (200), 64.37° (220), and 77.34° (311) representing the face centered cubic structure of silver (JCPDS file no. 89-3722). In comparison to the other three facets, the strong reflection at 111, may perhaps signify the growth path of the nanocrystals [45]. The average crystalline size of the AgNPs formed in the bioreduction was determined using the Scherrer equation and is estimated as 78 nm. The intense XRD pattern thus undoubtedly shows that AgNPs formed by the reduction of Ag^+ ions using *L. nodiflora* aqueous extract are crystalline in nature. Similar results were reported for AgNPs in the literature [46–48].

The morphology of synthesized AgNPs was confirmed by SEM analysis. They were approximately spherical in shape with smooth surface (Fig. 4a). Due to its spherical nature, the synthesized particles were found to be highly scattered and the shape of the particles has correlated with SPR band at 442 nm for AgNPs. EDX is also very helpful as it provides elemental analysis or chemical characterization of a sample. By measuring the energy and intensity of X-rays, qualitative and quantitative elemental analysis can be estimated. The chemical composition of nanoparticles synthesized from aerial extract of *L. nodiflora* was examined using EDX in SEM. The presence of nanocrystalline elemental silver was confirmed by the optical absorption peak, which is observed approximately at 3 keV. The EDX spectrum indicates strong silver signal followed by Cl peak almost at 2.5 keV. The Cl signal observed in EDX spectra may be originated from the plant extract (Fig. 4b).

The zeta potential of the particles robustly depends on the pH and the electrolyte concentration of the dispersion [49]. Even though, the zeta potential is higher than 30 mV or lesser than −30 mV, the dispersion is found to be stable in practice. In our study, AgNPs dispersed in physiological saline was extremely stable with a zeta potential value of −25.2 mV (Fig. 5a). Moreover, the negative charge of particles has a propensity to afford more stable particles by preventing them from agglomeration process [50]. Thus, our result supports the above information. The average particle size measured by DLS was 143.7 nm as shown in Fig. 5(b). This may be due to the detection of minor amounts of large sized particles produced by agglomeration or contamination, which caused uncertainties in particle sizes. The size measured by DLS analysis was higher than that measured by TEM analysis. The significant differences in both analysis probably reveals that TEM purely measures a number based size distribution of the physical size and does not consist of any capping agent, whereas DLS measures the hydrodynamic diameter (diameter of the particle) along with ions or molecules that are attached to the surface and moves with the AgNPs in solution [51]. Hence, these ions or other associated molecules create the particle to show larger to the instrument in comparison to TEM.

The structural morphology and size of synthesized AgNPs were further characterized by TEM micrograph images (Fig. 6). Fig. 6(a) and (b) clearly shows the spherical structure of AgNPs, which is in agreement with the shape of SPR band recognized from the UV-visible spectrum. The TEM readings displayed that the particles are well dispersed in nature with a size range of 30–60 nm and found to be highly crystalline as shown by clear lattice fringes and selected area electron diffraction (SAED) pattern (Fig. 6c).

3.2. Evaluation of antioxidant properties of AgNPs

The DPPH scavenging activities are recognized to be due to the hydrogen donating abilities of antioxidants. The result of different concentrations of AgNPs on DPPH radical scavenging activity is shown in Fig. 7(a). Both AgNPs and BHT established a significant inhibitory activity against the DPPH radical and thereby signify a source for antioxidants. The free radical scavenging activity of AgNPs tends to increase with increasing its concentration. Notably, AgNPs exhibit stronger antioxidant activity of 67% at 500 µg/ml. However, the standard BHT demonstrated 83% inhibition in the same concentration. The probable DPPH scavenging activity of AgNPs reported previously has supported the results of our present study [52–54].

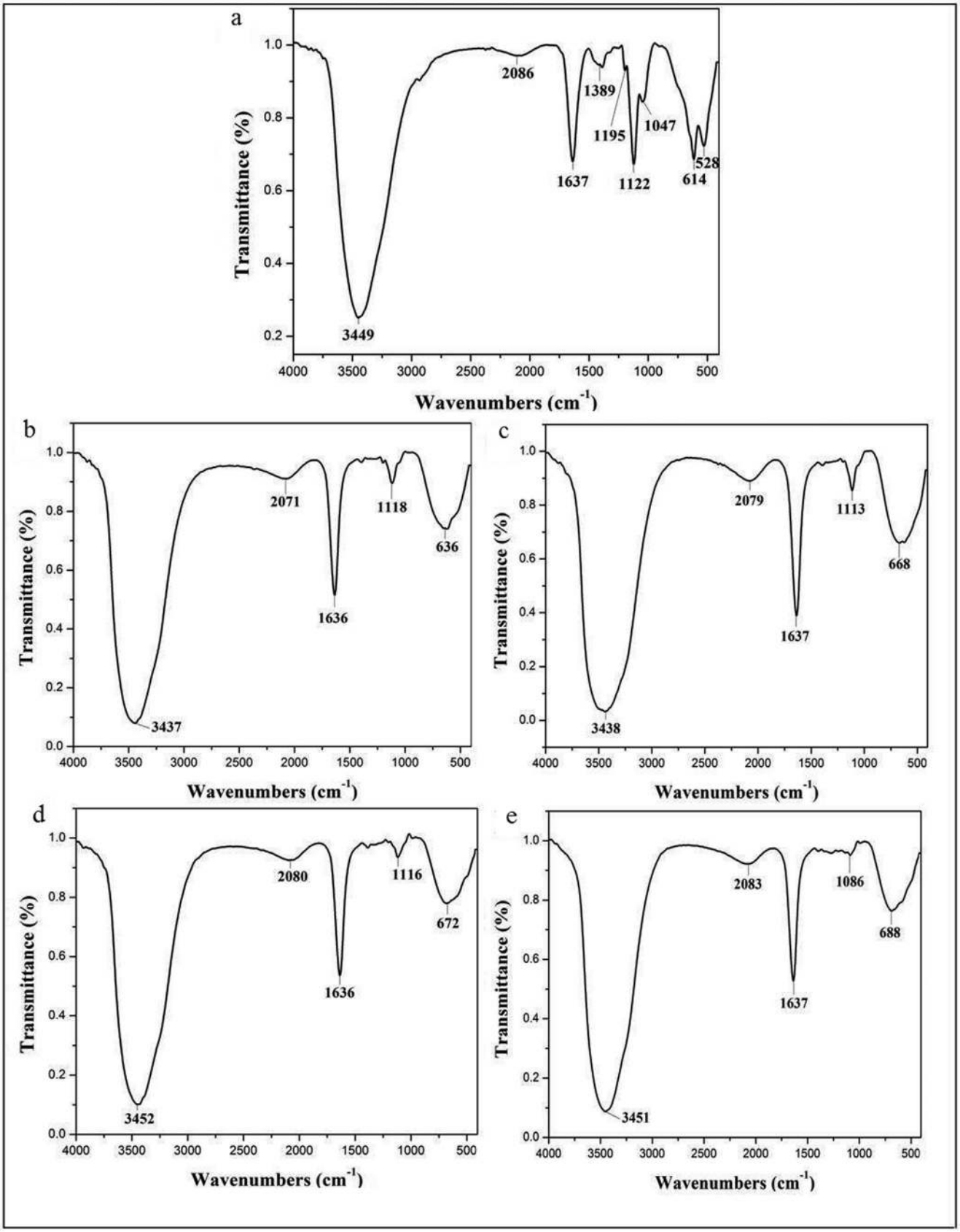

Fig. 2. FTIR spectra of AgNPs synthesized using *L. nodiflora* extract. (**a**) FTIR peak of aqueous plant extract, (**b**) intense of FTIR band shift at 30 °C, (**c**) intense of FTIR band shift at 60 °C, (**d**) intense of FTIR band shift at 90 °C, (**e**) intense of FTIR band shift at 95 °C.

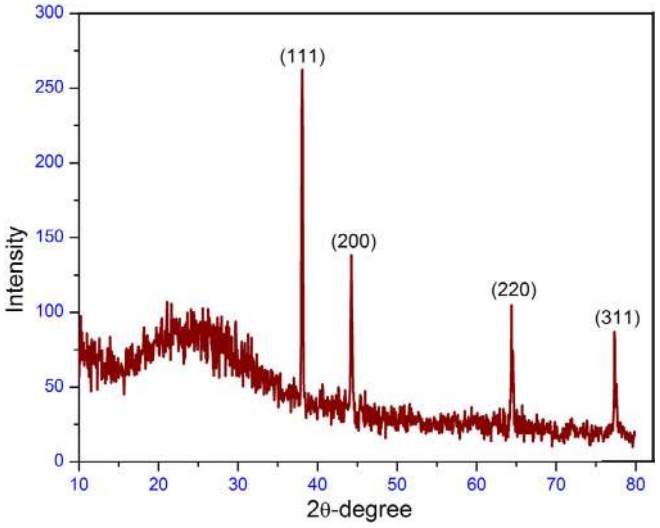

Fig. 3. XRD pattern of prepared AgNPs exhibiting the facets of crystalline silver.

The superoxide anion radical is recognized to be very injurious to cellular components as a herald of more reactive oxygen species, contributing to tissue damage and various diseases [55]. In this study, the superoxide radical scavenging activity of AgNPs and BHT is shown in Fig. 7(b). The inhibition percentage of superoxide radical was increased correspondingly with increasing the quantity of sample. The maximum inhibition of superoxide radical scavenging activity was about 70% by AgNPs as compared to the activity of BHT (84%) at the concentration of 500 µg/ml. Therefore, superoxide radical-scavenging activity by AgNPs as antioxidants has many physiological implications. Similar interpretations with potential superoxide scavenging activity by gold and AgNPs have been reported earlier [20].

The hydroxyl radical (˙OH) radical is one of the principal component in the progression of carcinogenesis, mutagenesis, and cytotoxicity, by means of causing DNA damages [56]. The AgNPs scavenged ˙OH radical in a concentration-dependent manner, as shown in Fig. 8(a). The scavenging ability of AgNPs was significant at all tested concentrations with maximal inhibition of 69% at 500 µg/ml whereas, BHT as a positive control was highly effective on hydrogen radical scavenging with 75% activity at 500 µg/ml. The experimental result of AgNPs, to scavenge or inhibit the ˙OH radical signifies that the AgNPs could significantly inhibit lipid peroxidation because ˙OH radicals are well concerned in peroxidation process.

The reducing ability of a substance may serve as a principal marker of its prospective antioxidant activity. Fig. 8(b) shows the reductive power of AgNPs relative to BHT, a well known antioxidant. The AgNPs revealed comparatively enhanced reducing power than BHT and the reducing activity of AgNPs was found to increase with increasing concentrations. At the concentration of 500 µg/ml, the reducing power of AgNPs and BHT was 0.115 and 0.095, respectively. It is also noteworthy that AgNPs shows consistently higher reducing power than those acquired for DPPH scavenging activity. Our interpretation was found to be similar to the observations made by Dipankar and Murugan [57] for AgNPs synthesized from *Iresine herbstii* leaves.

H_2O_2 is measured as one of major inducers of cellular aging and could attack numerous cellular energy-producing systems [58]. The AgNPs and BHT exerted concentration-dependent H_2O_2 scavenging activities, as depicted in Fig. 8(c). At the concentration of 500 µg/ml, the H_2O_2 scavenging activity for AgNPs and BHT was 71.1% and 68.2%, respectively. However, AgNPs exhibited higher H_2O_2 scavenging activity than BHT. The results herein suggest that AgNPs was an excellent platform to scavenge the ROS and there is an immense potential for the biologically synthesized AgNPs as a natural basis of antioxidants.

3.3. Antibacterial activity of biosynthesized nanoparticles

In this study, the antibacterial activity of AgNPs synthesized from *L. nodiflora* and its extract was evaluated by disc diffusion assay against five different bacterial species. AgNPs exhibited strong antibacterial activity against all tested bacterial pathogens at 50 µg/ml concentration (Fig. S1) and the growth inhibition zone values were calculated in millimeter (mm) (Table 1). As shown in Table 1, AgNPs has exposed highest zone of inhibition of about 24.1 mm for *S. pneumonia* followed by *E. coli* (22 mm). Both *S. aureus* and *K. pneumonia* showed similar antibacterial activity. The *L. nodiflora* aerial extract did not show any zone of inhibition at

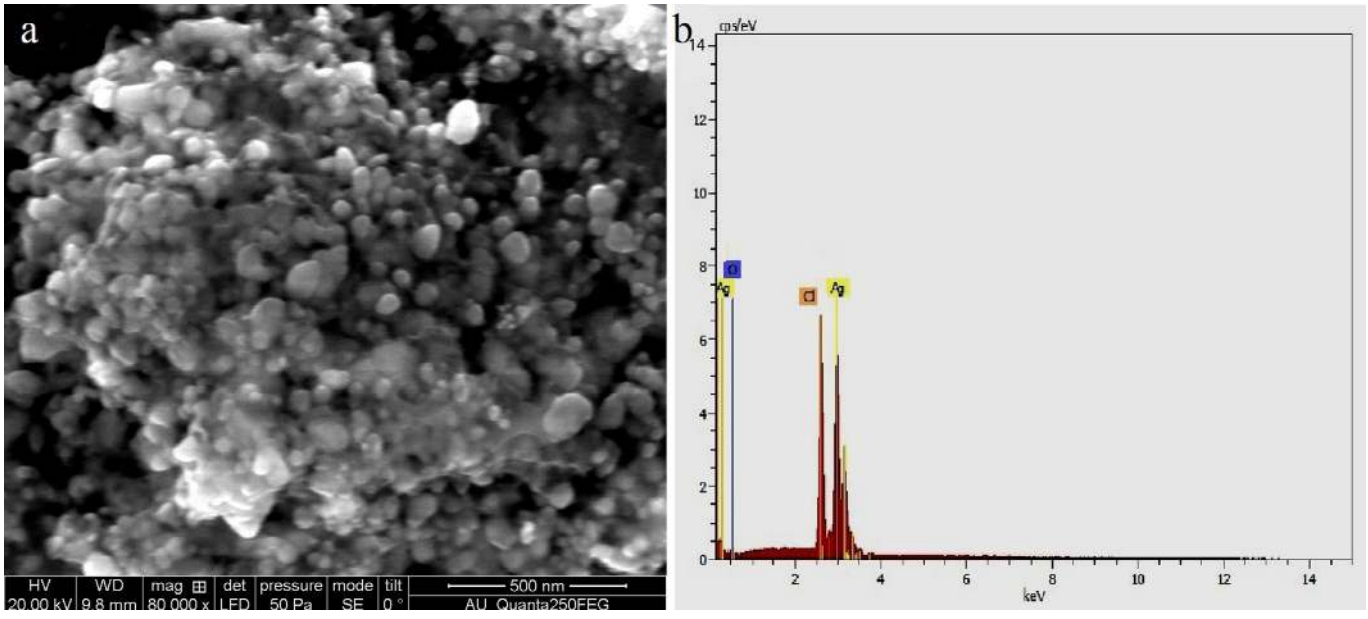

Fig. 4. (**a**) SEM micrograph of AgNPs and (**b**) EDX spectra of AgNPs synthesized by aerial extract established silver as main composition of the nanoparticles.

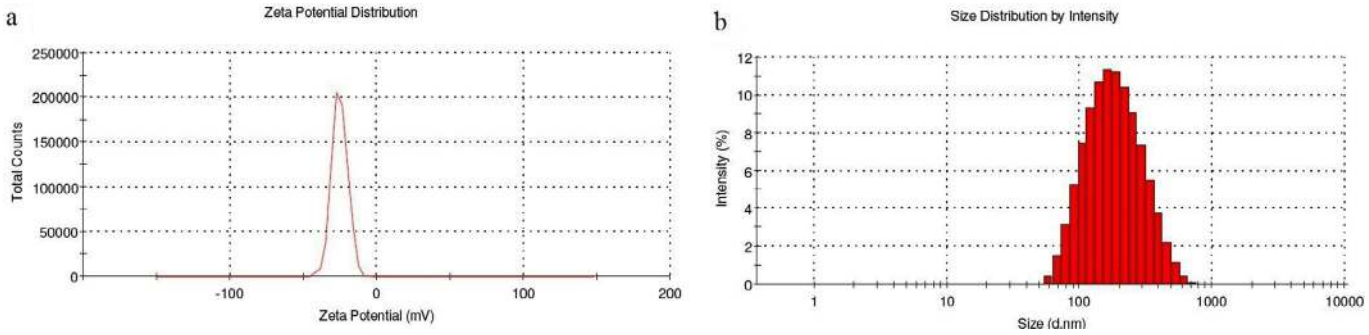

Fig. 5. (**a**) Stable AgNPs at −25.2 mV in zeta potential analysis and (**b**) Size distribution of AgNPs with maximum intensity at 143.7 nm.

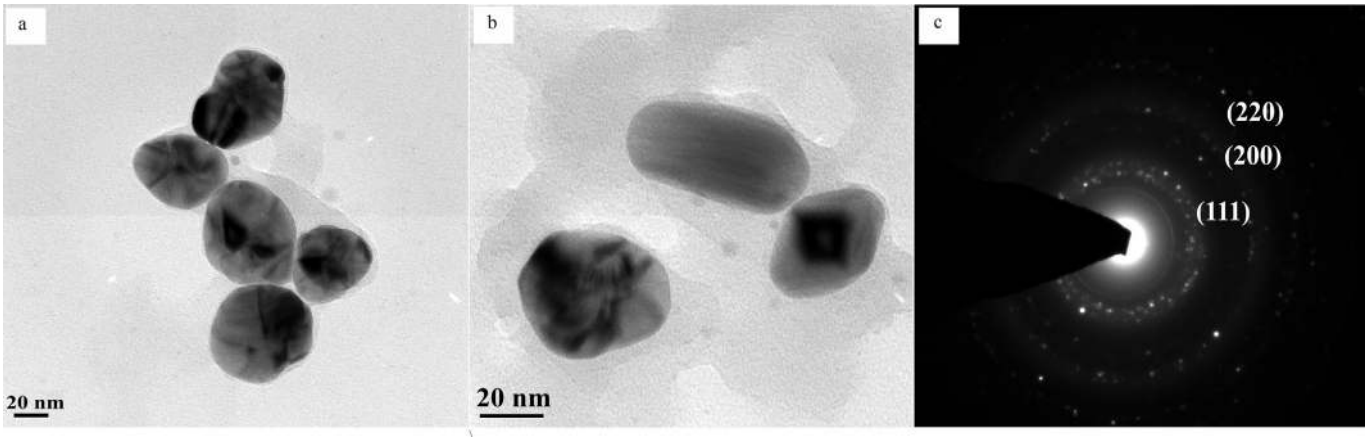

Fig. 6. (**a, b**) TEM images of AgNPs observed at 20 nm scale and (**c**) selected area electron diffraction (SAED) pattern of AgNPs.

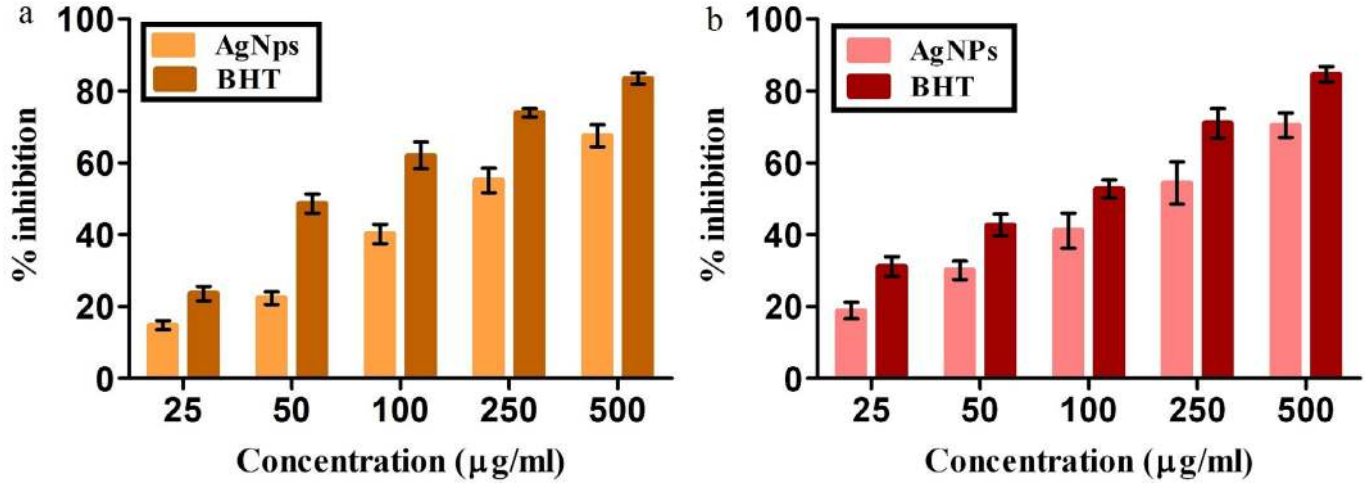

Fig. 7. Antioxidant efficacy of AgNPs using DPPH radical (**a**) and Superoxide radical (**b**) scavenging assays.

Table 1
Antibacterial activity of aerial extract and silver nanoparticles of *L. nodiflora*.

Test sample	Concentration (µg/ml)	Inhibition zone diameter (mm)				
		S. aureus	*S. mutans*	*S. pneumonia*	*E. coli*	*K. pneumonia*
Plant extract	50	–	–	–	–	–
AgNPs	50	20.3 ± 0.32	18.2 ± 1.2	24.1 ± 0.9	22.0 ± 1.5	20.4 ± 0.76

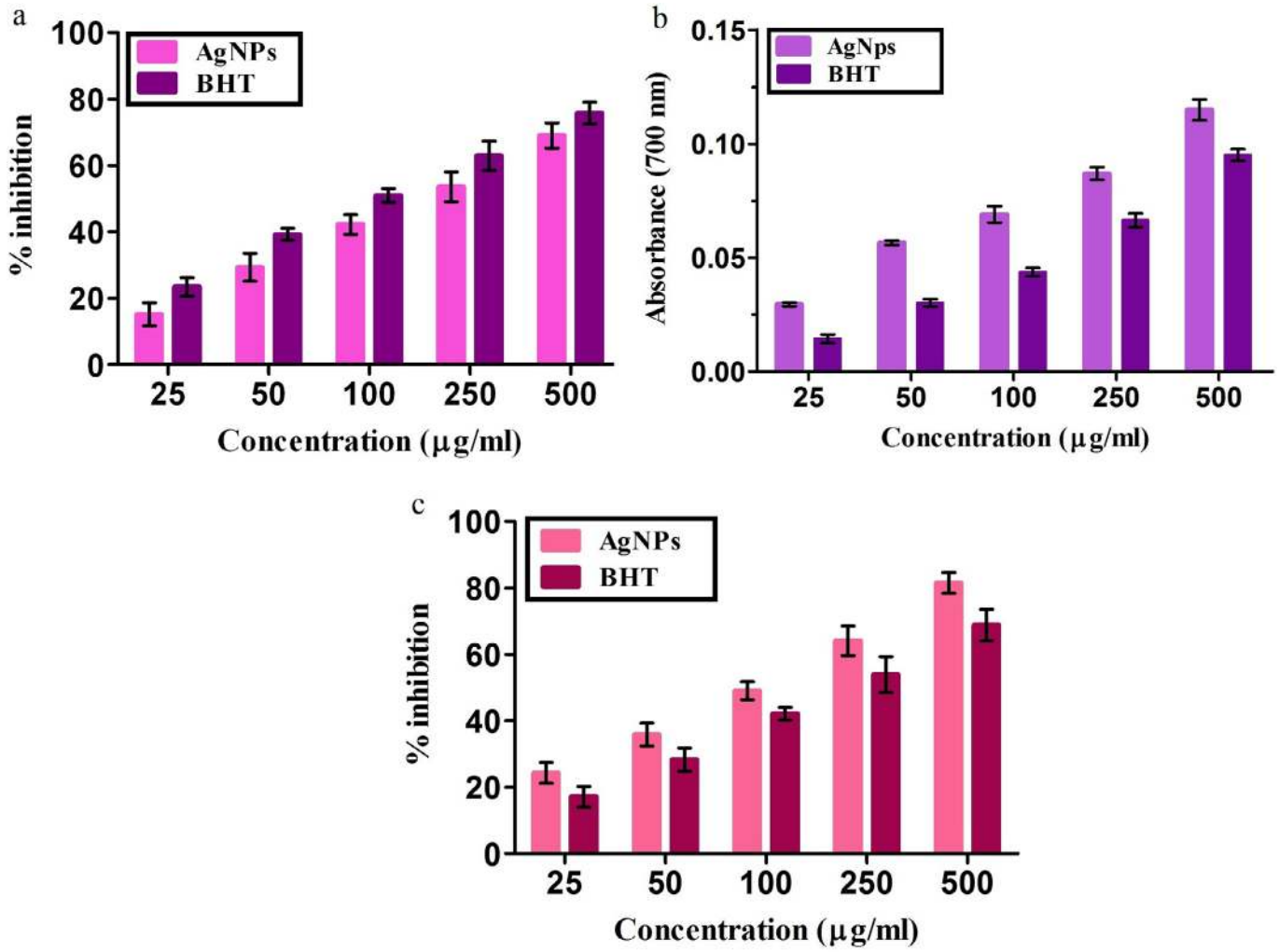

Fig. 8. Antioxidant activity of AgNPs using hydroxyl radical (**a**), reducing power (**b**), and hydrogen peroxide (**c**) assays.

the tested concentration. On the other hand, after formation of nanoparticles, the suspension has exposed significant antibacterial activity against bacterial pathogens. From the results, it can be noted that, *S. pneumonia* was more sensitive towards AgNPs than other pathogens. Previous studies signified that AgNPs are extremely known for its antibacterial activity against many gram positive and gram negative bacteria [57,59]. Recently, But, the selectivity for diverse bacterial strains changes owing to the presence of capping agents and stabilizers used in the preparation of AgNPs. The higher activity of AgNPs may conceivably due to the conformational changes persuaded in the membrane structure of bacterial cell wall by the action of AgNPs resulting in increased membrane permeability, and as a result leads to bacterial cell death [60].

3.4. In vitro cytotoxicity and morphological observation

The cytotoxic effects of synthesized AgNPs against cancer cell lines were highlighted in several literatures. In the present investigation, the anticancer efficacy of biosynthesized AgNPs was studied against MCF-7 cell line and the percentage of cell viability of AgNPs are illustrated in Fig. 9(a). The cytotoxicity effect was found to be increased with increase in concentration of AgNPs. The AgNPs inhibited the cell growth by 3.9, 11.8, 23.5, 56.9 and 72.8% at doses of 5, 10, 25, 50 and 100 µg/ml, respectively. Hence, the cytotoxicity induced by biosynthesized AgNPs in the treated cells, correspondingly resulted in the inhibitory concentration (IC_{50}) value of 40 µg/ml after 24 h treatment. The morphological changes were examined in both untreated and treated MCF-7 cells, under phase contrast microscope. It was found that the untreated MCF-7 (control) cells exhibited a high confluence of monolayer cells and a smooth, flattened morphology with intact cell membrane (Fig. 9b). Whereas, the AgNPs treated cells exhibited retraction, rounding, detachment from the surface and suspended cells were apparently accumulated. These results suggest that AgNPs can induce cell death in MCF-7 cells and our finding is reliable with the earlier reports [61].

4. Conclusion

In this present study, we conclude that, AgNPs were successfully synthesized from the aqueous extract of the aerial parts of *L. nodiflora* as a reducing and capping agents. The structural, morphological and elemental studies of biologically synthesized AgNPs were fully characterized by UV-visible spectroscopy, FTIR, XRD, SEM, EDX and TEM respectively. The synthesized AgNPs are crystalline in nature and exhibit a sharp SPR band width at 442 nm. TEM showed the formation of AgNPs with an average size of 30–60 nm. The biomedical efficacy of the characterized nanoparticles was efficiently determined using antioxidant, antimicrobial and anticancer properties. The biosynthesized AgNPs exhibited strong antioxidant activity of about 71% in scavenging H_2O_2. Hence, the synthesized nanoparticles may provide potential applications as free

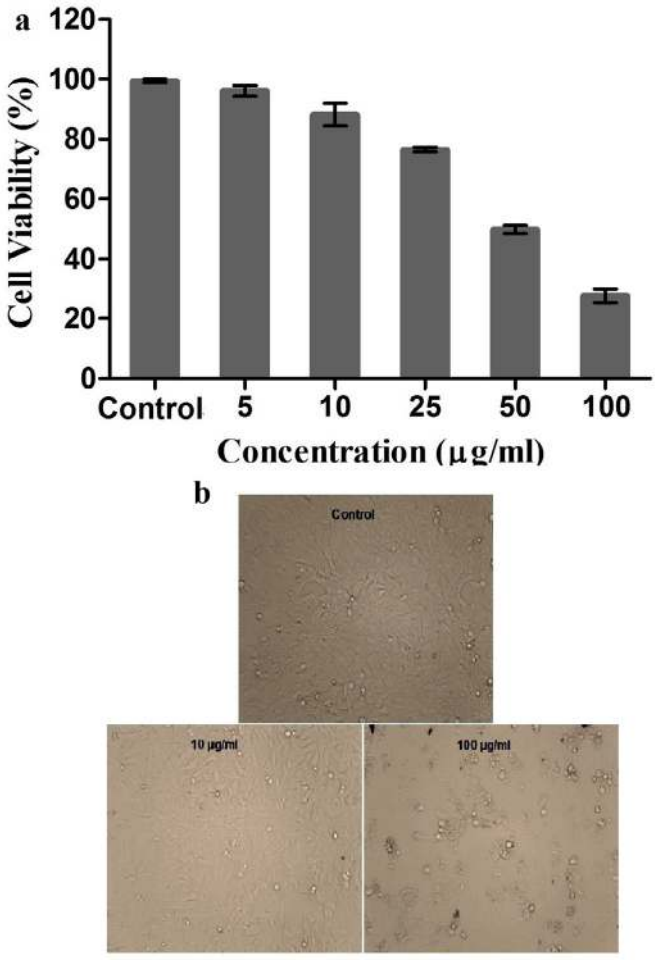

Fig. 9. (**a**) Cell viability of AgNPs on MCF-7 cells analyzed by MTT method (**b**) Morphological alterations of untreated (control) and treated MCF-7 cells (10 µg/ml; 100 µg/ml).

radical scavengers in treatment of various diseases. Moreover, AgNPs might be useful for the progress of newer and more effective antimicrobial and anticancer agents. From these studies, it can be inferred that nanoparticles biosynthesis may possibly be a gateway to our various health concerns.

Acknowledgements

The authors gratefully thank the School of Physics, Alagappa University for extending the XRD facility and also the Department of Industrial Chemistry, Alagappa University for providing the SEM with EDX facilities.

Conflict of Interest

The authors declare that they have no conflict of interest.

Supplementary materials

Supplementary material associated with this article can be found, in the online version, at doi:10.1016/j.reffit.2017.07.002.

References

[1] M.C. Roco, W.S. Bainbridge, J. Nanopart. Res. 7 (2005) 1–13.
[2] K. Yokohama, D.R. Welchons, Nanotechnology 18 (2007) 105101–105107.
[3] N.T. Kaushik, S.M. Snehit, Y.P. Rasesh, Nanomed. Nanotechnol. Bio. Med. 6 (2010) 257–262.
[4] A.K. Mittal, A. Kaler, U.C. Banerjee, Nano Biomed. Eng. 4 (2012) 118–124.
[5] A.K. Mittal, Y. Chisti, U.C. Banerjee, Biotechnol. Adv. 31 (2013) 346–356.
[6] B. Kumar, K. Smita, L. Cumbal, BioNanoSci. 6 (2016) 15–21.
[7] N.J. Reddy, D. Nagoor Vali, M. Rani, S. Sudha Rani, Mat. Sci. Eng. C 34 (2014) 115–122.
[8] M. Ghaedi, M. Yousefinejad, M. Safarpoor, H. Zare Khafri, M.K. Purkait, J. Ind. Eng. Chem. 31 (2015) 167–172.
[9] V.P. Manjamadha, K. Muthukumar, Bioprocess Biosyst. Eng. 39 (2016) 401–411.
[10] P. Velmurugan, M. Cho, S. Lim, S. Seo, H. Myung, K. Bang, S. Sivakumar, K. Cho, B. Oh, Mater. Lett. 138 (2015) 272–275.
[11] P. Velmurugan, K. Anbalagan, M. Manosathyadevan, K. Lee, M. Cho, S. Lee, J. Park, S. Oh, K. Bang, B. Oh, Bioprocess Biosyst. Eng. 37 (2014) 1935–1943.
[12] S. Ahmed, M.Ahmad Saifullah, B. L.Swami, S. Ikram, J. Radiat. Res. Appl. Sci. 9 (2016) 1–7.
[13] P.R.R. Sre, M. Reka, R. Poovazhagi, M.A. Kumar, K. Murugesan, Spectrochim. Acta 135 (2015) 1137–1144.
[14] M.R. Bindhu, M. Umadevi, Spectrochim. Acta A 135 (2015) 373–378.
[15] N. Hermans, P. Cos, L. Maes, T. De Bruyne, D.Vanden Berghe, A.J. Vlietinck, L. Pieters, Curr. Med. Chem. 14 (2007) 417–430.
[16] G. Agati, E. Azzarello, S. Pollastri, M. Tattini, Plant Sci. 196 (2012) 67–76.
[17] F. Dajas, J. Ethnopharmacol. 143 (2012) 383–396.
[18] S.M. Nabavi, S.F. Nabavi, W.N. Setzer, H. Alinezhad, M. Zare, A. Naqinezhad, J. Diet Suppl. 9 (2012) 285–292.
[19] L. Du, S. Suo, G. Wang, H. Jia, K.J. Liu, B. Zhao, Y. Liu, Chemistry 19 (2013) 1281–1287.
[20] C.H. Ramamurthy, M. Padma, I.D. Samadanam, R. Mareeswaran, A. Suyavaran, M.S. Kumar, K. Premkumar, C. Thirunavukkarasu, Colloids Surf. B Biointerfaces 102 (2013) 808–815.
[21] K.P. Upendra, S.S. Preeti, S. Anchal, Dig. J. Nanomater. Biostruct. 4 (2009) 159–166.
[22] P.K. Stoimenov, R.L. Klinger, G.L. Marchin, K.J. Klabunde, Langmuir 18 (2002) 6679–6686.
[23] C. You, C. Han, X. Wang, Y. Zheng, Q. Li, X. Hu, H. Sun, Mol. Biol. Rep. 39 (2012) 9193–9201.
[24] Chapter 03 B. Kumar, K. Smita, B. Kumar, in: James C. Taylor (Ed.), Advances in Chemistry Research, Volume 37, Nova Science Publishers, USA, 2017, pp. 87–120. Chapter 03.
[25] H.R. Vasanthi, S. Mukherjee, I. Lekli, D. Ray, G. Veeraraghavan, D.K. Das, J. Cardiovasc. Pharmacol. 53 (2009) 499–506.
[26] S. Mutheeswaran, P. Pandikumar, M. Chellappandian, S. Ignacimuthu, J. Ethnopharmacol. 137 (2011) 523–533 .R.
[27] R. Dodoala, B. Divit, K. Koganti, V.S.R.G Prasad, Indian J. Nat. Prod. Resour. 1 (2010) 314–321.
[28] A. Sudha, P. Srinivasan, Int. J. Pharm. Sci. Res. 4 (2013) 4263–4271.
[29] T. Yamaguchi, H. Takamura, T. Matoba, J. Terao, Biosci. Biotechnol. Biochem. 62 (1998) 1201–1204.
[30] M. Nishikimi, N.A. Rao, K. Yagi, Biochem. Biophys. Res. Commun. 46 (1972) 849–853.
[31] G.C. Yen, H.Y. Chen, J. Agr. Food Chem. 43 (1995) 27–32.
[32] R.J. Ruch, S.J. Cheng, J.E. Klaunji, Carcinogenesis 10 (1989) 1003–1008.
[33] I. Hinneburg, H.J.D. Dorman, R. Hiltunen, Food Chem. 97 (2006) 122–129.
[34] F.A. Tomás-Barberán, J.B. Harborne, R. Self, Phytochemistry 26 (1987) 2281–2284.
[35] S. Siddiqui, F. Ahmed, S.K. Ali, S. Perwaiz, S. Begum, Nat. Prod. Res. 23 (2009) 436–441.
[36] M.R. Bindhu, M. Umadevi, Spectrochim. Acta A 101 (2013) 184–190.
[37] S.P. Chandran, M. Chaudhary, R. Pasricha, A. Ahmad, M. Sastry, Biotechnol. Prog. 22 (2006) 577–583.
[38] K. Vijayaraghavan, S.P. Kamala Nalini, N. Udaya Prakash, D. Madhankumar, Colloids Surf. B 94 (2012) 114–117.
[39] Z. Zaheer, Rafiuddin, Colloids Surf. B 90 (2012) 48–52.
[40] J.J. Antony, M. Nivedheetha, D. Siva, G. Pradeepha, P. Kokilavani, S. Kalaiselvi, A. Sankarganesh, A. Balasundaram, V. Masilamani, S. Achiraman, Colloids Surf. B 109 (2013) 20–24.
[41] E. Kelly, L. Coronado, L. Zhao, G.C. Schatz, J. Phys. Chem. B 107 (2003) 668–677.
[42] J. Kong, S. Yu, Acta Biochim. Biophys. Sin. 39 (2007) 549–559.
[43] J. Huang, Q. Li, D. Sun, Y. Lu, Y. Su, X. Yang, H. Wang, Y. Wang, W. Shao, N. He, J. Hong, C. Chen, Nanotechnology 18 (2007) 105104–105115.
[44] T. Klaus, R. Joerger, E. Olsson, G.C. Granqvist, Proc. Natl. Acad. Sci. U.S.A. 96 (1999) 13611–13614.
[45] D. Philip, Spectrochim. Acta A 78 (2011) 327–331.
[46] S. Barua, R. Konwarh, S.S. Bhattacharya, P. Das, K.S. Devi, T.K. Maiti, M. Mandal, N. Karak, Colloids Surf. B 105 (2013) 37–42.
[47] K.B. Narayanan, N. Sakthivel, Colloids Surf. A 380 (2011) 156–161.
[48] A.K. Mittal, J. Bhaumik, S. Kumar, U.C. Banerjee, J. Colloid Interf. Sci. 415 (2014) 39–47.
[49] C. Jacobs, R.H. Müller, Pharmaceut. Res. 19 (2002) 189–194.
[50] U. Suriyakalaa, J.J. Antony, S. Suganya, D. Siva, R. Sukirtha, S. Kamalakkannan, T. Pichiah, S. Achiraman, Colloids Surf. B 102 (2013) 189–194.
[51] H. Erjaee, H. Rajaian, S. Nazifi, Adv. Nat. Sci.: Nanosci. Nanotechnol. 8 (2017) 025004.
[52] J. Seralathan, P. Stevenson, S. Subramaniam, R. Raghavan, B. Pemaiah, A. Sivasubramanian, A. Veerappan, Spectrochim. Acta A. 118 (2014) 349–355.
[53] B. Kumar, A. Debut, K. Smita, L. Cumbal, Trans. Nonferrous Metals Soc. China 26 (2016) 2363–2371.
[54] B. Kumar, K. Smita, L. Cumbal, Nanotechnol. Rev. 6 (2016) 521–528.

[55] J. Nordberg, E.S. Arner, Free Radic. Biol. Med. 31 (2001) 1287–1312.
[56] M.A. Esmaeili, A. Sonboli, Food Chem. Toxicol. 48 (2010) 846–853.
[57] C. Dipankar, S. Murugan, Colloids Surf. B 98 (2012) 112–119.
[58] J. Liu, L. Jia, J. Kan, C.H. Jin, Food Chem. Toxicol. 51 (2013) 310–316.
[59] B. Kumar, K. Smita, et al., in: S. Ranjan, et al. (Eds.), Nanoscience in Food and Agriculture 2, Sustainable Agriculture Reviews, Volume 2, chapter 7 Springer International Publishing, Switzerland, 2016, pp. 235–252. chapter 7.
[60] P. Dibrov, J. Dzioba, K.K. Gosink, C.C. Hase, Antimicrob. Agents Chemother. 46 (2002) 2668–2670.
[61] G. Babu, C. Arulvasu, D. Prabhu, R. Jegadeesh, R. Manikandan, Mater. Lett. 122 (2014) 98–102.